Contents lists available at GrowingScience

Engineering Solid Mechanics

homepage: www.GrowingScience.com/esm

Hydrolysis effect on the mechanical resistance on impact cycles in polyamide multifilaments

Felipe Teixeira Spilka[a], Daniel Magalhães da Cruz[a,b*], Maurício de Oliveira Silva[a] and Carlos Eduardo Marcos Guilherme[a]

[a]*Stress Analysis Laboratory Policab, Engineering School (EE), Federal University of Rio Grande (Furg), 96203-000, Rio Grande/RS, Brazil*
[b]*Applied Mechanics Group (GMAp), Department of Mechanical Engineering (DEMEC), Federal University of Rio Grande do Sul (UFRGS), 90050-170, Porto Alegre/RS, Brazil*

ARTICLEINFO

Article history:
Received 18 July 2024
Accepted 26 January 2025
Available online
26 January 2025

Keywords:
Experimental Characterization
Dynamic Loads
Polyamide Fibers
Hydrolysis Depolymerization
Sudden Loads
Mechanical Behavior

ABSTRACT

Offshore moorings play a key role in the stability of maritime structures such as floating oil production platforms. This study focuses on polyamide as a promising alternative for offshore moorings due to its mechanical characteristics and degradation resistance. Initially, characterization tests are carried out to determine the polyamide's linear density, the rupture strength, and the linear tenacity. Following, impact tests are carried out on polyamide samples, using a methodology based on a free fall mass effect. The analysis of the results includes statistical data filtering and the parameterization of curves to correlate the number of impact cycles to the applied load. Furthermore, the effect of the accelerated hydrolysis on polyamide is investigated, subjecting the samples to an aging process in fresh water for 180 days at 65°C. The results are analyzed to evaluate the effect of the hydrolysis on the resistance to impact cycles. It was concluded that, in general, polyamide shows a promising ability for energy absorption and impact resistance, with the potential for its use in offshore moorings. However, it is necessary to consider the hydrolysis effect on the degradation of its mechanical properties over time. This study contributes to the advancement of knowledge about the performance of polyamide in marine environments, providing important insights for the design and maintenance of offshore mooring systems, and also contemplating an exploratory study for its material's behavior.

© 2025 Growing Science Ltd. All rights reserved.

1. Introduction

Offshore moorings represent an essential part of maritime infrastructure, ensuring the stability and safety of marine structures (Chakrabarti, 2005; Rudman & Cleary, 2016), such as the FPSO - floating production storage and offloading units. Among the widely used mooring systems is the Taut-Leg, known for its effectiveness in distributing loads and reducing excessive platform movements (Wang, 2022). This system is incorporated into synthetic fiber moorings that play a crucial role, offering mechanical resistance, flexibility for commissioning and/or decommissioning, and durability under adverse maritime conditions.

Del Vecchio (1992) attested that polyester fibers were an excellent solution for anchoring systems, today this same fiber is presented in the literature as an established choice for offshore mooring. Its tensile strength and the ability to resist degradation caused by prolonged exposure to marine elements make the polyester fiber a reliable option for offshore applications. It also is an excellent cost-effective solution and especially attractive for large-scale projects. (McKenna, Hearle & O'Hear, 2004; Bastos & Silva, 2020).

This context allowed the evolutionary study of several other fibers, such as high modulus polyethylene (HMPE), aramid, polyacrylate, polypropylene, and others. From this extensive list, a promising alternative that has gained prominence is polyamide, also known as nylon. This synthetic fiber has several important advantages, including an exceptional energy absorption capacity, flexibility, abrasion resistance, and high tenacity (Najafi, Nasri & Kotek, 2017; Militký, Venkataraman & Mishra, 2018). Furthermore, polyamide demonstrates a remarkable resistance to fatigue, thus extending the life span of the moorage and reducing maintenance costs over time. These characteristics make polyamide an attractive and versatile option

* Corresponding author.
E-mail addresses: dacruz.daniel@furg.br // daniel.cruz@ufrgs.br (D.M. da Cruz)

ISSN 2291-8752 (Online) - ISSN 2291-8744 (Print)
© 2025 Growing Science Ltd. All rights reserved.
doi: 10.5267/j.esm.2025.1.006

for the rigorous demands of the offshore sector, complementing and, in some cases, surpassing the polyester qualities in certain applications (Ma, Jin & Zhang, 2018; Sozen, Coskun & Sahin 2023).

Polyamide multifilaments have been widely explored for floating offshore wind turbines (FOWT) due to the need to use a low modulus material because of the characteristics of the wave mechanics in shallow waters (low installation depths) ranging from 50 to 100 meters depth (Chevillotte *et al.*, 2020). It is noteworthy that this material is also used in climbing sports applications due to its low longitudinal stiffness, which allows the rope to deform to the point of not transmitting great efforts to the climber's body in the event of a fall, prioritizing the user's safety (McLaren, 2006; Arrieta *et al.*, 2013).

In addition to the mentioned properties, polyamides have high rupture strength (Chevillotte *et al.*, 2020), good chemical resistance, and good flexibility (Arrieta *et al.*, 2013). On the other hand, its hygroscopic nature can lead to some limitations in its use, since its water absorption decreases by around 10% the tensile strength of the material (Weller *et al.*, 2015).

Thus, there is a certain tendency to study the effect of water associated with the depolymerization of its chains, specifically, it is called hydrolysis, as this phenomenon leads to a decrease in the material molecular weight, which leads to a decrease in its mechanical properties, mainly the tensile strength (Duarte *et al.*, 2019). As a hydrophilic material, polyamides are much more susceptible to attracting water molecules to their polymeric chain (McLaren, 2006). The aging caused by hydrolysis has already been previously studied (Jacques *et al.*, 2002), and a kinetic model was even created to predict the aging of the material in pure water. Fatigue of these multifilaments was also analyzed (Chevillotte *et al.*, 2020), concluding that the use of appropriate coatings resulted in a service life high enough not to be a limiting factor when applied for FOWT mooring.

Another factor to be considered is the use of these materials especially for applications where their dynamic and energy absorption aspects stand out. One of the possible loads in these applications is sudden or impact loads, which could degrade the fiber throughout its life span (Belloni *et al.*, 2022). During impact cycling, polyamide tends to lose its elasticity, increasing its stiffness until the material ruptures (da Cruz *et al.*, 2020). In this same study, the effect of impact loads on the mechanical behavior of the material was studied, observing that there was a decrease in impact resistance with the increase in the mass supported by the material in the test and that the immersion time in water decreased its resistance to impact cycles (da Cruz *et al.*, 2020).

Therefore, this article groups together hydrolysis and sudden loads, aiming to analyze the results for the resistance of impact cycles under different loads, with the effect of accelerated hydrolysis in polyamide multifilaments. In addition to the hydrolyzed results analyzed, it also compared the results obtained in the present study with similar results found in the literature that study impact cycling in polyamide multifilaments without the hydrolysis effect (in virgin condition).

2. Materials and Methods

2.1 Characterization Test and Materials

The material sample is polyamide in the form of multifilaments (yarns), the basic unit of an offshore mooring rope. Although it is not possible to disclose the sample manufacturing, it is noteworthy that the polyamide is taken from a virgin spool (**Fig. 1a**). Some tests are carried out for the initial characterization of the synthetic fiber, such as linear density tests (mass/length relationship), Yarn Break Load (YBL), and the determination of linear tenacity.

a) Polyamide spool

b) Precision scale OHAUS Adventurer

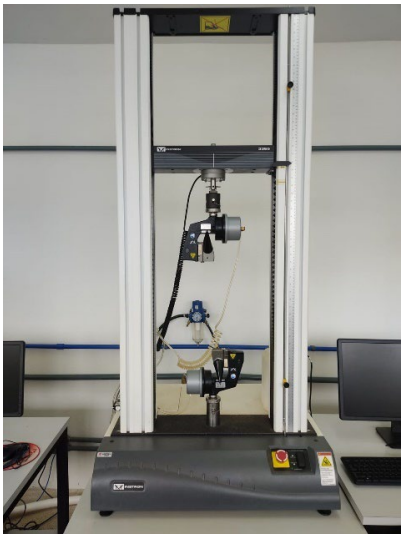

c) Instron 3365

Fig. 1. Material and equipment for initial characterization

The material linear density is defined with a series of mass-per-length measurements to obtain the mean and standard deviation, per ASTM D1577 (ASTM, 2018). Twenty test specimens with a standard-length of 1000 millimeters are used; After a 9-minute stabilization, the mass value is acquired with a precision scale (**Fig. 1b**), with the unit being a ratio of mass by length, usually tex (grams per kilometer).

The rupture test for the YBL complies with the ISO 2062 standard (ISO, 2009), being carried out on a universal testing machine (**Fig. 1c**). As for the sample quantity, 20 test specimens were used, manufactured with a standard-length of 1000 mm, without twisting. When fixed to the equipment, the effective length for testing is 500 mm, the rupture is then carried out at a constant extension rate of 250 mm/min. The unit of the data acquired is in force [N], and extension [mm].

The linear tenacity of the material is determined by the average results measured from the 20 specimens (linear density and rupture strength). It is calculated by dividing the rupture strength by the linear density, obtaining the linear tenacity [N/tex]. All tests are performed at temperatures and humidity that comply with ISO 139 (ISO, 2005), with a temperature of 20 ± 2°C and relative humidity of 65 ± 4%.

The results of this mechanical characterization are found in the literature (da Cruz *et al.*, 2020), and are presented in **Table 1**. These values (especially rupture strength) will be a reference for impact tests.

Table 1. Initial polyamide characterization, reference data

Material	Linear density [tex]	Rupture Strength [N]	Ruptura deformation [%]	Linear tenacity [N/tex]
Polyamide	284.6 ± 1.3	210.47 ± 3.78	16.61 ± 0.81	0.740 ± 0.017

2.2 Impact Tests Methodology

There are no specific standards for impact tests on multifilaments in the literature, making it difficult to perform the standard Charpy and Izod tests due to the specimen's flexibility and its geometric characteristics. Thus, the impact assessment uses free-fall masses, using a methodology based on the EN 892 standard (BSI, 2012) which standardizes impact tests on mountaineering ropes. **Fig. 2a** schematically represents the impact on free-falling ropes, where the variables are: rope length (l_0), free-fall height (h), mass (m), gravitational acceleration (g), and force $F(t)$ (Emri *et al.*, 2008; Nikonov *et al.*, 2011). **Fig. 2b** represents the impact apparatus built at the Policab Stress Analysis Laboratory and also used in other studies (da Cruz *et al.*, 2020; Belloni, Clain & Guilherme, 2021; Belloni *et al.*, 2022; Cruz *et al.*, 2023).

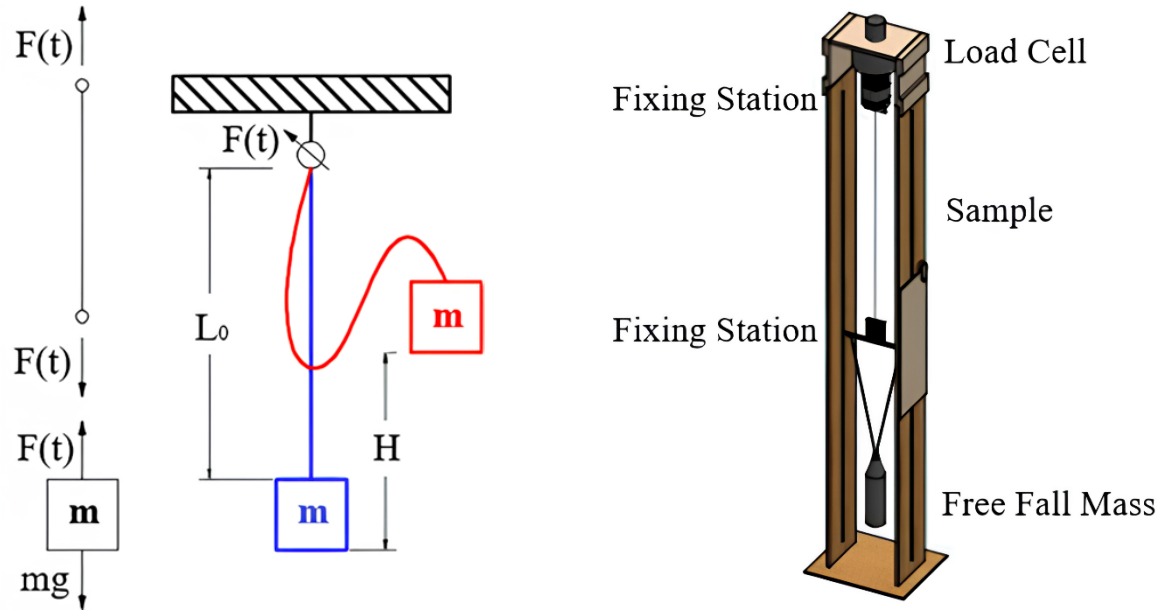

a) Free-fall schematics b) Scheme impact apparatus of Policab

Fig. 2. Schematic of the application of impact cycles and testing apparatus

For the impact test, samples were prepared with 500 mm length and at the ends with “sandwich” type terminations (clamping station). The mass is released from an initial free fall height of 300 mm, where this procedure is repeated until the complete rupture of the specimen. In addition to the number of resistant cycles for each sample, force per time data is also acquired by each cycle, using a load cell connected to the impact apparatus (**Fig. 3**). All impact tests are also performed in a standard controlled atmosphere for testing textile fibers (ISO, 2005).

Fig. 3. Load cell attached to the impact apparatus

Fig. 4. Hydrolysis tank at controlled temperature

Impact loads are based on the rupture strength of the multifilament. By dividing the value in Newtons by the gravity acceleration (g), a mass in kilograms is obtained that corresponds to 100% of the Yarn Break Load (YBL) of the multifilament. The load groups for impact coincide with the work of Cruz *et al.* (2023) to allow further comparisons. The load groups used for impact tests in the present work are: 3%, 4%, 5%, 6%, and 7% of the YBL, and their respective impact masses are shown in **Table 2**. For each load group, the sample quantity is 10 specimens.

Table 2. Impact loads and their respective free-fall masses

YBL [%]	Force [N]	Mass [kg]
100	210.47	21.462
3	6.31	0.644
4	8.42	0.858
5	10.52	1.073
6	12.63	1.288
7	14.73	1.502

2.3 Hydrolysis Condition

For the material condition, it was used hydrolysis aging (which is a depolymerization process), so the material remained in a freshwater reactor specially developed by Policab for a total time of 180 days. As the hydrolysis process is quite slow at room temperature, it was decided to accelerate the process by increasing the water temperature (Duarte *et al.*, 2019). Thus, the samples were immersed in a reactor with fresh water at a temperature of 65ºC (338.15K) at neutral pH. The reactor where the hydrolysis test was carried out is shown in **Fig. 4**.

After 180 days in hydrolysis, the multifilaments were removed from the reactor and the samples underwent a drying period in a room with controlled temperature and humidity, per ISO 139 standard (ISO, 2005). They remained in the room for two weeks before the impact tests were performed, a time considered sufficient for the multifilament to completely dry.

2.4 Results Analysis

2.4.1 Statistical Filtering

The analysis of the quantitative results of the impact cycles for rupture under each loading condition naturally needs to pass through statistical filtering. There are several statistical techniques for performing this analysis, some more sophisticated and mathematically robust, but in this case, the boxplot was chosen. Despite its simplicity, it is noteworthy that this technique suits very well the case of low sample size, one variable, distribution comparison, trends visualization, and variability (Schwertman, Owens, & Adnan, 2004; Montgomery & Runger, 2012).

Boxplot is an effective visual tool for summarizing the distribution of a data set, offering insights about its dispersion, and identifying possible outliers (Williamson, Parker, & Kendrick, 1989). It consists of a box representing the interquartile range (IQR), delimited by the first quartile (Q1) and the third quartile (Q3), with a central line that represents the median. Quartiles

are obtained by dividing the sorted data into four equal parts, while the IQR is calculated as the difference between Q3 and Q1. Outliers are points outside the range defined by 1.5 times the IQR above Q3 or below Q1. Mathematically, quartiles 1 and 3 can be expressed as shown in Eq. (1) and Eq. (2):

$$Q1 = percentile(data, 25\%) \tag{1}$$

$$Q3 = percentile(data, 75\%) \tag{2}$$

The interquantile range (IQR) is defined by Eq. (3), and the lower and upper limit, respectively, by Eq. (4) and Eq. (5).

$$IQR = Q3 - Q1 \tag{3}$$

$$limit_{min} = Q1 - 1.5 \times IQR \tag{4}$$

$$limit_{max} = Q3 + 1.5 \times IQR \tag{5}$$

These elements provide a compact and informative representation of the data distribution, allowing a rapid assessment of its variability and the presence of outliers.

2.4.2 Curve Parameterization

With the filtered data, it is possible to propose models that relate the average number of impact cycles to failure with the impact load (%YBL). The linearization of models associated with the Least Squares Method (MMQ) was proposed, in which the models analyzed were: linear, power, exponential, reciprocal, inverse adjustment, and Michaelis-Menten, **Table 3**. For curve adjustments, the best instrument for the quality measuring of each adjustment is the Determination Coefficient, (Gilat & Subramaniam, 2009), the closer R^2 is to 1, the better the adjustment.

Table 3. Curve adjustment, and linearization for MMQ

Model	Equation	
	Non-Linear Form	Linear Form
Linear	-	$y = B + Ax$
Power	$y = Bx^A$	$\ln y = \ln B + A \ln x$
Exponential	$y = Be^{Ax}$	$\ln y = \ln B + Ax$
Reciprocal	$y = \frac{1}{B + Ax}$	$\frac{1}{y} = B + Ax$
Michaelis-Menten	$y = \frac{Ax}{B + x}$	$\frac{1}{y} = \frac{1}{A} + \frac{B}{Ax}$

With the linearized models, from **Table 3**, the values of the coefficients A, and B are calculated by solving the linear equations system, Eq. (6) and Eq. (7). In this adjustment, the variable x is the percentage of the YBL subjected to the impact loading, and the variable y is the number of impact cycles to failure. The amount of data is n, and the coefficients A and B are the results obtained for each one of the models. The adjustment was made with the help of the free Octave software (https://octave.org/), using a script available in the literature (Cruz *et al.*, 2024).

$$A \cdot n + B \cdot \sum x_i = \sum y_i \tag{6}$$

$$A \cdot \sum x_i + B \cdot \sum x_i^2 = \sum x_i \cdot y_i \tag{7}$$

2.4.3 Impact Cycles Analysis

The load cell attached to the impact equipment (**Fig. 3**) can provide important results in terms of force and time, allowing the analysis of the impact cycles. Through the acquired data, the unit described by the area under the graph (force multiplied by time) is an impulse unit [N×s]. Although the unit is not a measure of energy, the impact is caused by the gravitational potential energy, and this force-time graph may be able to indicate the energy absorption capacity. It is possible to plot the force versus time graph, as shown in **Fig. 5**.

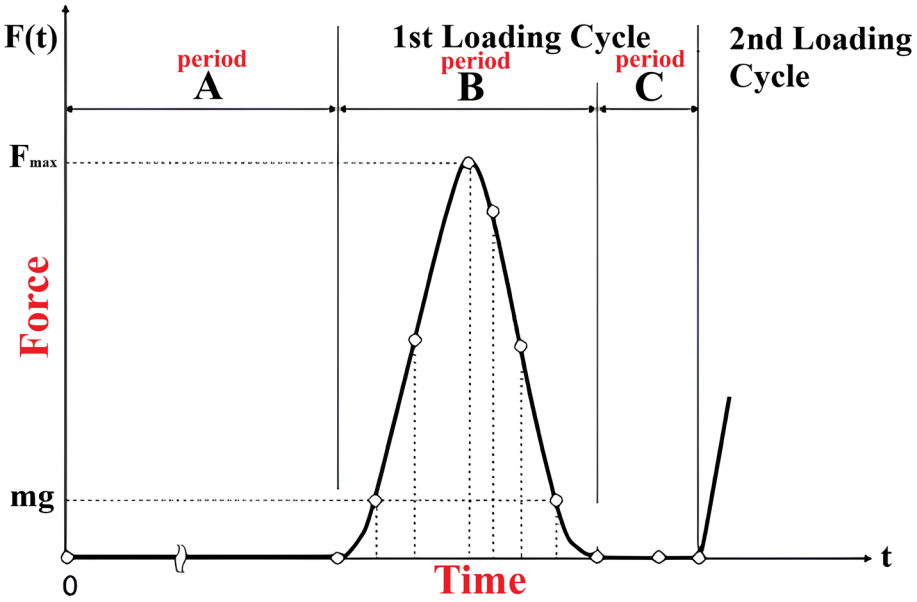

Fig. 5. Theoretical graph of force versus time.

The first phase (Period A) of this graphic corresponds to a zero load, as the mass is in free fall and there will be no force registered in the load cell. The second phase (Period B) characterizes the rope deformation process, where this sudden loading occurs. The third phase (Period C) is a moment of zero load but with an upward movement of the mass, known as ricochet (Emri *et al.*, 2008). After the mass falls again, the first phase restarts, but with a significantly lower peak force than the previous one. This is repeated continuously until there is no energy for ricochets, then if the sample does not rupture, the load stabilizes at a value corresponding to the product of the mass by gravity.

3. Results and Discussion

For the results of the impact cycles on polyamide under hydrolysis, it is obtained for each of the 5 load groups, 10 cycling values for the respective sample group. Results are shown for the total data in **Table 4** and as well for the mean and the standard deviation (SD).

Table 4. Cycling Results for the rupture impact

CP	3% YBL	4% YBL	5% YBL	6% YBL	7% YBL
1	56	8	8	3	1
2	25	8	11	3	2
3	27	7	5	5	1
4	42	15	8	3	5
5	21	10	4	4	2
6	27	11	4	2	2
7	15	11	8	3	3
8	14	8	12	3	5
9	21	16	5	8	2
10	36	10	3	8	4
Max	56	16	12	8	5
Min	14	7	3	2	1
Mean	28.4	10.4	6.8	4.2	2.7
Standard Deviation	12.98	3.03	3.08	2.15	1.49

All groups had their data filtered by the statistical criteria shown in section 2.4.1. There were practically no values outside the upper and lower limits for each load group. The only exception was specimen number 9, from the 4% YBL group (highlighted in red, in **Table 4**). As a result, all the filtered averages remain unchanged, except for the 4% YBL group, where the filtered average is 9.78, replacing the unfiltered average of 10.40. **Table 5** shows all the filtering statistical quantities and the graphical constructions of all boxplots (**Appendix A**).

Table 5. Statistical quantities for data filtering by boxplot

	3% YBL	4% YBL	5% YBL	6% YBL	7% YBL
$Q1$	21	8	4	3	2
$Q3$	36	11	8	5	4
IQR	15	3	4	2	2
$limit_{min}$	-1.5	3.5	-2	0	-1
$limit_{max}$	58.5	15.5	14	8	7
Outliers	-	16	-	-	-
Average Filtering	28.40	9.78	6.80	4.20	2.70

With the filtered data and the averages established for the resistance in the impact cycles in polyamide multifilaments submitted to hydrolysis conditions, it is possible to compare with literature results made for polyamide in normal conditions under the same free-fall masses (Cruz *et al.*, 2023). **Table 6** presents the average results for both conditions, where the deleterious effect on the mechanical behavior of the hydrolysis process is evident.

Table 6. Resistance to impact cycles in polyamide fibers: hydrolysis and virgin condition

Impact Load [%YBL]	[kg]	Normal (Cruz *et al.*, 2023)	Hydrolysis (present work)	Relation Hydrolysis /Reference
3	0.644	330.4	28.4	0.086
4	0.858	48.8	9.78	0.2
5	1.073	30	6.8	0.227
6	1.288	22.2	4.2	0.189
7	1.502	6.6	2.7	0.409
8	1.717	4.2	-	-
9	1.932	2.2	-	-

It is noteworthy how the group with the lowest impact mass (3%YBL) significantly differs, showing a cycling amount 11 times greater for virgin polyamide than for polyamide in hydrolysis conditions. While the other groups present a less discrepant difference, of up to 5 times the impact cycle value for virgin polyamide when compared to hydrolysis. It is worth highlighting that the 8% and 9% YBL groups, although presented in the reference for virgin polyamide, were not submitted for the hydrolysis condition as all 10 specimens ruptured after just one cycle, and it would not be possible to state which is the limiting condition factor for rupture in a single cycle. For visualization, **Fig. 6** presents the data compiled in a bar graph, comparing the virgin and hydrolysis conditions of the five load groups in the present study.

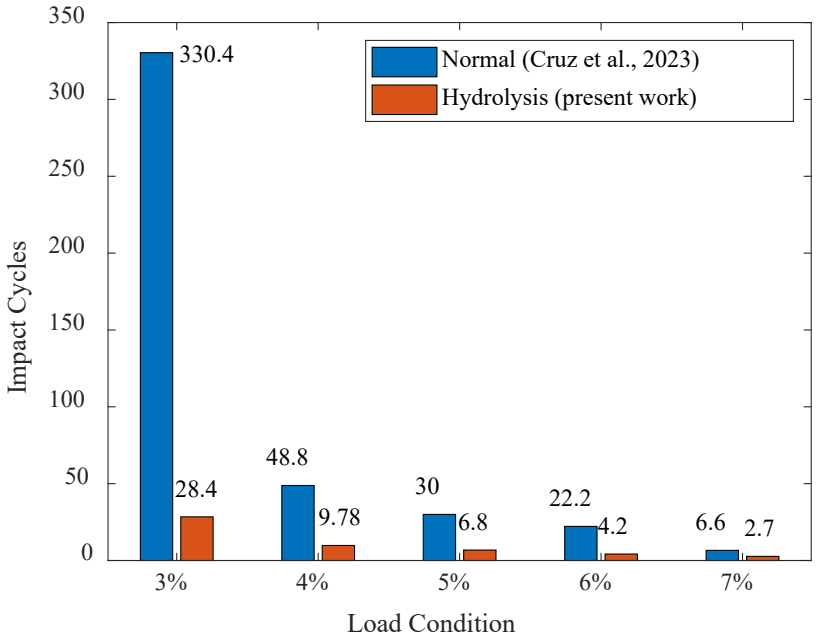

Fig. 6. Comparative graph of impact cycle in virgin condition and hydrolysis

With the data filtered for the hydrolysis condition, it is natural to build mathematical models that describe the relationship between the two variables (impact cycle versus load). Applying the methodology described in topic 2.4.2, the data is adjusted for 5 different models, with the results shown in **Table 7**.

Table 7. Curves adjustment for different models, impact cycles on polyamide with hydrolysis

Model	A	B	R^2	Equation Form
Linear	-5.698	38.866	0.746	$y = B + Ax$
Power	-2.664	476.867	0.984	$y = Bx^A$
Exponential	-0.555	117.938	0.954	$y = Be^{Ax}$
Reciprocal	0.081	-0.225	0.960	$y = \frac{1}{B + Ax}$
Michaelis-Menten	1.921	-3.006	0.829	$y = \frac{Ax}{B + x}$

Using the best determination coefficient criteria, the adjustment that best represents the impact cycle data in polyamide under hydrolysis is the power model, Eq. (8).

$$y = 476.867x^{-2.664} \tag{8}$$

When comparing the curve adjustment results obtained by Cruz *et al.* (2023), it is noted that the power model also shows the best results. Eq. (9) displays the model obtained in the referenced work for impact cycles in polyamide without hydrolysis. Both adjustments, Eq. (8) and Eq. (9), are plotted together and also with an indication of the discrete data in **Fig. 7**.

$$y = 29235.60x^{-4.27} \tag{9}$$

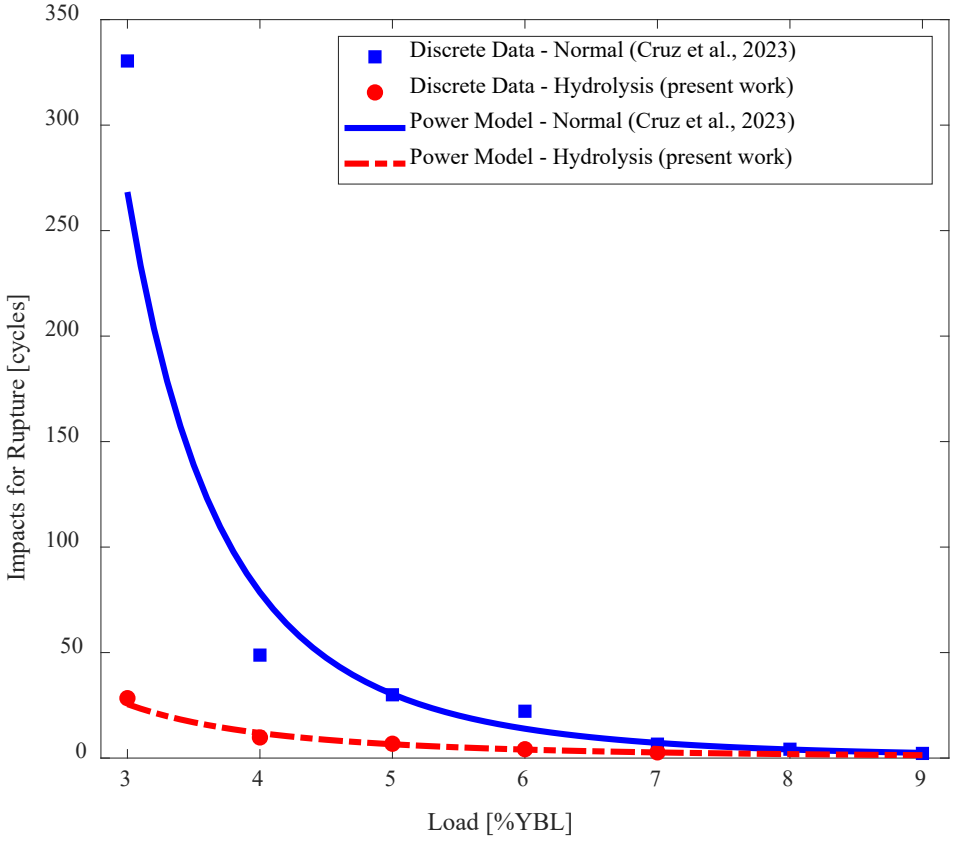

Fig. 7. Adjustment curves for discrete data, impact on normal polyamide submitted to hydrolysis

All data are presented coherently, indicating that hydrolysis reduces the impact resistance of polyamide multifilaments. In a way, this was already an expected result but until then the reduction proportion still needed to be discovered.

A fundamental point must be explored based on this feeling of an "expected result". This is because, for any mechanical test, hydrolyzed conditions naturally have a lower performance when compared to the same material under normal conditions. And if you look at the impact masses used, they are based on a virgin rupture of polyamide multifilaments. So perhaps, the reduction is not necessarily in the behavior under impact cycles, but rather for any mechanical test on the multifilament under hydrolysis conditions, and even more so, perhaps considering the reduction in rupture resistance caused by hydrolysis, the resistance to impact cycles remains similarly proportional to the condition without hydrolysis.

To study the possibility of this effect, rupture tests were performed for the hydrolysis condition. For the virgin condition, as shown in **Table 1**, the polyamide rupture strength (virgin) was 210.47 Newtons, and the rupture strain was 16.61%. After the rupture tests were carried out for polyamide with hydrolysis, the rupture resistance showed a significant drop of almost 25%, where the rupture force presented on average was 158.55 Newtons, and the rupture deformation reduced by approximately 9%, recording average values of 15.12%. **Fig. 8** shows the force versus deformation behavior for polyamide in both conditions: with hydrolysis and without hydrolysis.

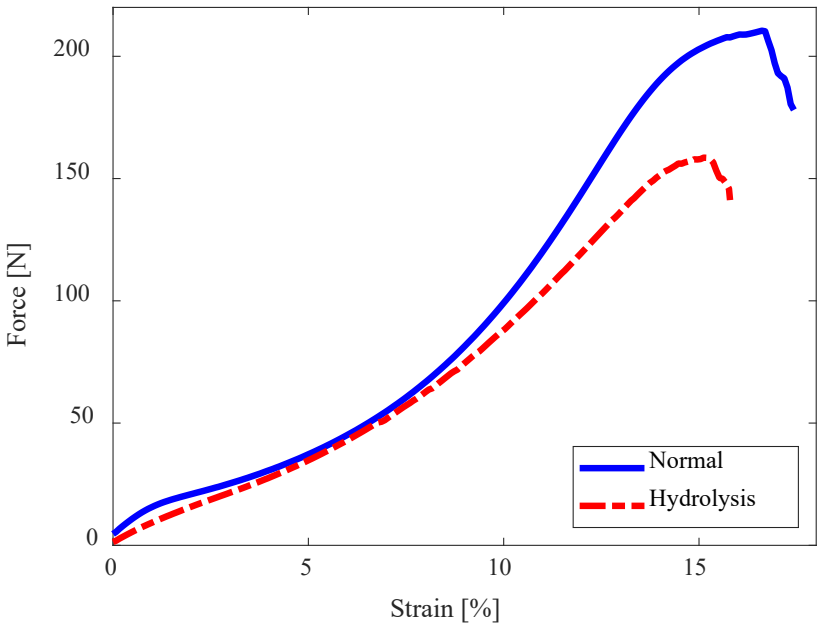

Fig. 8. Rupture charts for polyamide multifilaments with and without hydrolysis

Rupture with hydrolysis presents a worse performance from the perspective of mechanical resistance, which also presents another characteristic curve of the fiber's constitutive behavior. Using this rupture value as a reference (158.55 N), it is possible to redetermine the appropriate impact percentages to which each of the used free fall masses referred for the impact cycles, **Table 8**.

Table 8. Readjustment of free fall masses with indication of the respective percentage of YBL

YBL without hydrolysis [%]	Impact masses	Equivalent Force [N]	YBL with hydrolysis [%]
3	0.644	6.31	3.98
4	0.858	8.42	5.31
5	1.073	10.52	6.64
6	1.288	12.63	7.97
7	1.502	14.73	9.29

With the new Yarn Break Load percentage correspondences in hydrolysis condition readjusted by the rupture with hydrolysis value, data shown again in **Table 9**, the curve adjustment for the new YBL percentage relation can be done again. The power adjustment was once again the best method for the five models, with the corresponding adjustment being presented in Eq. (10).

Table 9. Resistance to impact cycles readjusted by rupture with hydrolysis

Impact Load		Impact cycles for rupture
[%YBL]	[kg]	
3.98	0.644	28.4
5.31	0.858	9.78
6.64	1.073	6.8
7.97	1.288	4.2
9.29	1.502	2.7

$$y = 1010.563 \cdot x^{-2.662} \tag{10}$$

Thus, it is possible to replot the adjustment curves with the discrete data, **Fig. 9**, now adding the model and the values readjusted by the rupture value with hydrolysis.

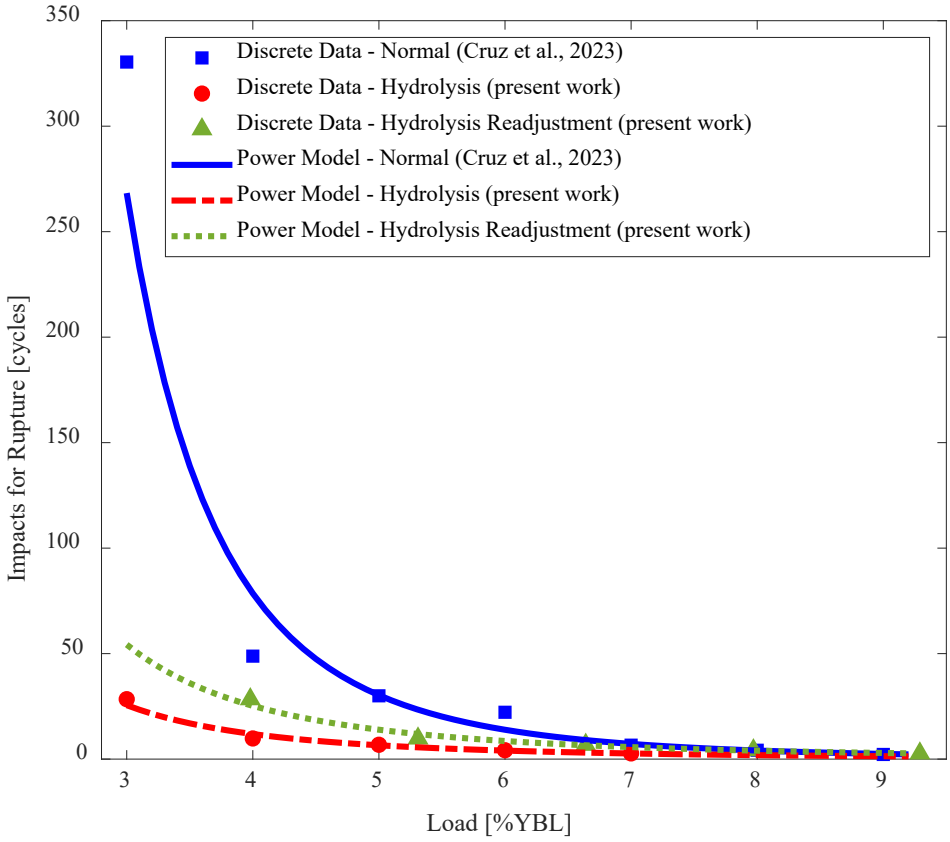

Fig. 9. Fitting curves for discrete data, impact on normal polyamide (blue), with hydrolysis (red), and readjusted through rupture with hydrolysis (green)

At first, it may seem like a graphical reconstruction and a disjointed data interpretation, especially placing the percentages of rupture loads in a way that does not coincide with the reference work studied for polyamide without hydrolysis (Cruz *et al.*, 2023). However important understandings can be drawn from the graphic reconstruction presented in **Fig. 9**. Therefore, if by reducing the rupture mechanical resistance through hydrolysis, and by readjusting the model to the new data, if the green curve is very close to the blue curve, this would mean that even with a decrease in rupture, the impact cycle resistance characteristics would not change if a proportional scale to the rupture value of the tested condition is considered.

Thus, the fact that the readjusted curve (green and dotted curve in **Fig. 9**) is visibly not coincident with the other curves, and it is also between the other two curves, demonstrates that:

- Using the virgin polyamide rupture reference for impact cycles with hydrolysis creates an instantaneous decrease in the impact cycle resistance versus the load (dotted curve in green above the dash-dot curve in red);
- There is a natural reduction in mechanical resistance resulting from the depolymerization of the hydrolysis process (both in terms of rupture and impact cycle resistance), but the hydrolysis condition also presents a worsening, proportionally speaking, in the impact cycle resistance (curve dotted in green below the solid curve in blue);

Thus, it is clear that hydrolysis reduces impact cycle resistance, both when it is placed absolutely (dash-dot curve in red) and when placed relatively (dotted curve in green). This indicates that the impact cycle resistance is not only modified by the hydrolyzed conditions but also by other effects of dynamic loads such as cycling loads. A behavior that reinforces this is the change in the constitutive response in rupture with and without hydrolysis, **Fig. 8**.

For the results acquired by the load cell, in terms of time and force, it should be noted that they are noisy data, sensitive to the data acquisition frequency, and sensitive mainly to the test execution itself (parallax error related to the operator). Therefore, the graphical analysis was avoided for the loads that came to rupture with fewer cycles. This is so that the changes in behavior can be perceived and understood throughout the cycles.

As it is unfeasible to make an average in each impact cycle with the entire sample, it was decided to determine the closest characteristic specimen to the average group. For impact cycles at 4% YBL, the established filtered average was 9.78, with the characteristic specimen being specimen 5 (10 cycles to rupture). The 10 cycles for rupture by impact with a load of 4% YBL are represented in **Fig. 10**, in this figure, the cycles are slightly out of phase, so that the load peaks are graphically non-coincident and arranged side by side to facilitate the visualization of their variations throughout the cycles.

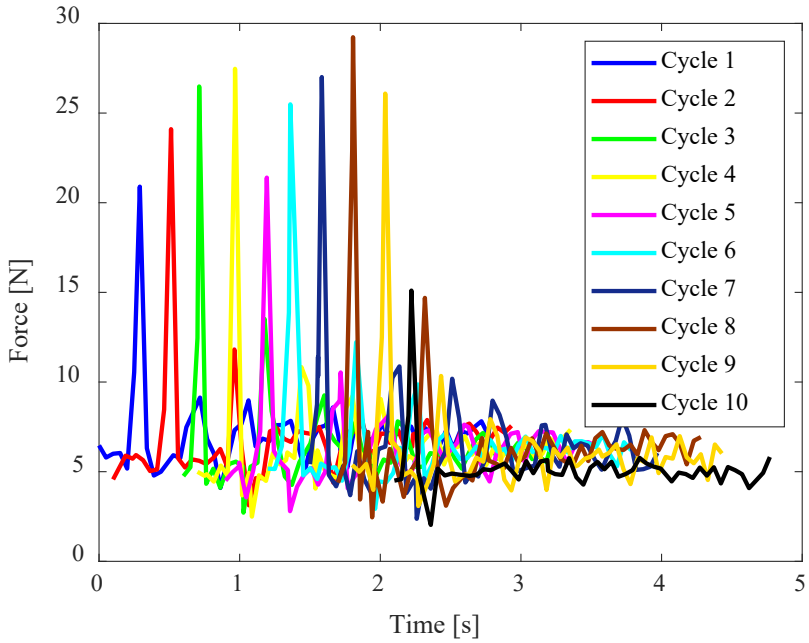

Fig. 10. Impact cycles to rupture, force *versus* time, 4% YBL specimen 5

It can be seen that the maximum force captured tends to increase, although for this group there is some inconsistency when comparing cycle 4 (in light yellow) with cycle 5 (in magenta). But what draws attention is the low force value in the rupture cycle of cycle 10 (in black), because, in the same graph shown in **Fig. 10**, the maximum force in the tenth cycle resembles the same force value in the first ricochet of cycle 8, which is approximately half the scale magnitude of the other force peaks in the other cycles.

This mentioned behavior was particularly observed in other samples from the same load group, and for other load groups. This means that impact cycles increase the material tenacity, up to a limit condition, which does not always coincide exactly with a theoretical maximum force peak, depending on the cycling, the load history can leave the sample in its penultimate cycle in a very tenuous condition where virtually any impact stress will cause the specimen to rupture.

Aiming for an overview of the behavior that occurs throughout the cycles, it is interesting to analyze specimen 1 with a load condition of 3% of the YBL, this is because, among the entire sample set, it is the specimen that most resists impact cycles (reaching rupture in the 56th cycle). Graphing all 56 cycles would be very confusing, precisely because of the data concentration and its noise, so **Fig. 11**, which presents the data, is constructed with cycles 1, 10, 19, 33, 51, and 55.

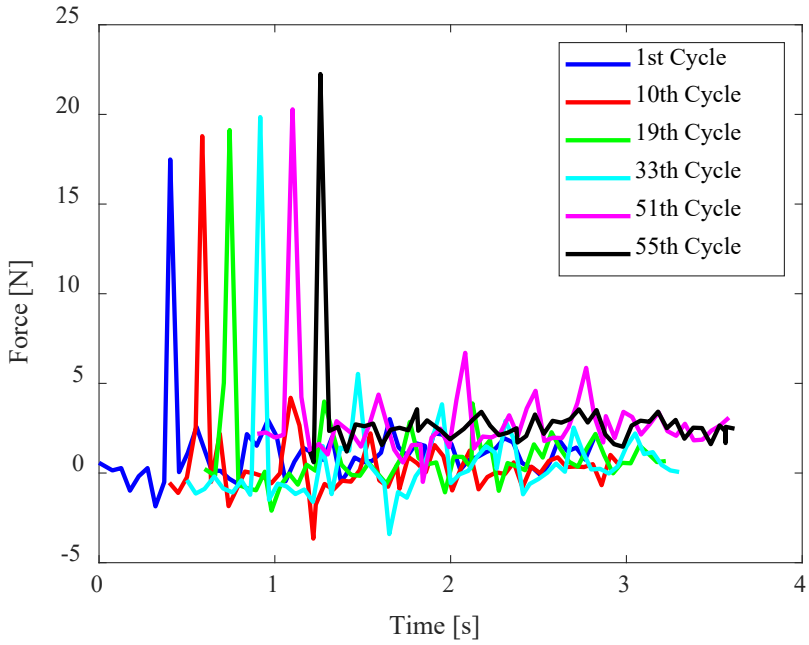

Fig. 11. Impact cycles for rupture, force versus time, 3% YBL specimen 1

Note that the last curve (55th cycle, in black) is not the cycle in which the rupture occurs. This is because the rupture occurs in the following cycle, the 56th cycle, but when the data is captured, it does not present a significant peak of force, being confused with noise, which is a confirmation of the same finding obtained in **Fig. 10**, that the limit condition of tenacity imposed on the sample is in most cases determined by the penultimate impact cycle.

In **Fig. 11**, the gradual increase in the maximum force acquired throughout the cycles can be seen. Polyamide is naturally a material with high elongation compared to other synthetic fibers, when submitted to a certain mechanical load, depending on the loads, even if there is an elastic recovery (understood in impact cycling as ricochet), a portion of the permanent deformation (plastic deformation) remains in the sample. When the impact cycles are re-executed, the free fall height becomes the same 300 mm (as in the first cycle) added to the plastic deformation cycle by cycle. It is very difficult to measure the specimen plastic deformation, as it is still an incipient aspect of this determination, but the progressive behavior of the maximum imposed force, as well as its stabilization throughout the test, and the maximum peak value close to the limit condition for rupture by impact demonstrates precisely this progression of plastic deformation in concomitance with an increase in the sample stiffness, up to the failure condition.

4. Conclusion

This study investigated the hydrolysis effects on the resistance of impact cycles in polyamide multifilaments. The results indicate a clear reduction in the mechanical resistance of materials subjected to hydrolysis compared to materials under normal conditions. This decrease is evident in all load groups tested, with an average reduction in the resistance to impact cycles of up to five times compared to a virgin polyamide multifilament.

Comparison with previous studies also highlights the harmful effect of hydrolysis on the mechanical behavior of polyamide multifilaments. The analysis of the rupture data revealed a significant drop in the tensile strength of the hydrolyzed materials (approximately 25% at rupture).

When adjusting the resistance data from the impact cycles to consider the reduction in tensile strength due to hydrolysis, it was observed that the ratio between the hydrolyzed and non-hydrolyzed conditions did not remain relatively proportional. This suggests that in addition to the hydrolysis causing an absolute reduction in mechanical resistance, it also causes a relative reduction in the impact cycle performance. This is an indication of the need to investigate these effects for other types of dynamic loads.

The data also revealed interesting patterns in the materials' behavior throughout impact cycles. Notably, the sample reaches its tenacity limit condition frequently in its penultimate impact cycle, before the rupture occurs. Furthermore, a gradual progression in the material stiffness was observed throughout the cycles, accompanied by a stabilization in the maximum imposed force.

These results highlight the importance of considering not only the material absolute mechanical resistance but also its behavior under dynamic conditions, such as the impact cycles. Future research may benefit from further analysis of the interactions between hydrolysis and other aspects of the mechanical behavior of polyamide multifilaments, as well as the development of more accurate test methods to assess plastic deformation over impact cycles. Furthermore, improving both the testing methodology and the analysis of the results by coupling analytical modeling to experimentally acquired data would be a promising possibility for study.

Acknowledgments

This study was financed in part by the Coordenação de Aperfeiçoamento de Pessoal de Nível Superior – Brasil (CAPES) – Finance Code 001.

References

American Society for Testing and Materials. (2018). D1577-07 Standard Test Methods for Linear Density of Textile Fibers. ASTM: West Conshohocken.

Arrieta, C., Dong, Y., Lan, A., & Vu-Khanh, T. (2013). Outdoor weathering of polyamide and polyester ropes used in fall arrest equipment. *Journal of Applied Polymer Science, 130*(5), 3058-3065. https://doi.org/10.1002/app.39524

Bastos, M. B., & Silva, A. L. N. (2020, May). Evaluating Offshore Rope Fibers: Impact on Mooring Systems Integrity and Performance. In Offshore Technology Conference. OTC-30830-MS. https://doi.org/10.4043/30830-MS

Belloni, E. S., Clain, F. M., & Guilherme, C. E. M. (2021). Post-impact mechanical characterization of HMPE yarns. *Acta Polytechnica, 61*(3), 406–414. https://doi.org/10.14311/AP.2021.61.0406

Belloni, E. S., Monteiro da Fonseca Thomé da Silva, A. H., Clain, F. M., & Marcos Guilherme, C. E. (2022). Fatigue and impact load: Experimental investigation on mechanical behavior of high modulus polyethylene yarns. *Polymers and Polymer Composites, 30*, 09673911221103934. https://doi.org/10.1177/09673911221103934

British Standards Institution. (2012). EN 892 Mountaineering Equipment-Dynamic Mountaineering Ropes: Safety Requirements and Test Methods. BSI: London.

Chakrabarti, S. (2005). Handbook of Offshore Engineering (2-volume set). Elsevier.

Chevillotte, Y., Marco, Y., Bles, G., Devos, K., Keryer, M., Arhant, M., & Davies, P. (2020). Fatigue of improved polyamide mooring ropes for floating wind turbines. *Ocean Engineering, 199*, 107011. https://doi.org/10.1016/j.oceaneng.2020.107011

Cruz, D. M., Melito, I., Cruz Júnior, A. J., Sales, M. W. R., Popiolek Júnior, T. L., & Guilherme, C. E. M. (2024). Desenvolvimento de código aberto em Octave para ajustes de funções através de linearização e MMQ. *E&S Engineering and Science, 13*(1), 16896. https://doi.org/10.18607/ES20241316896

Cruz, D. M., Silva, A. H. M. F. T., Clain, F. M., & Guilherme, C. E. M. (2023). Experimental study on the behavior of polyamide multifilament subject to impact loads under different soaking conditions. *Engineering Solid Mechanics, 11*(1), 23-34. https://doi.org/10.5267/j.esm.2022.11.001

da Cruz, D. M., Belloni, E. S., Clain, F. M., & Guilherme, C. E. M. (2020). Analysis of impact cycles applied to dry polyamide multifilaments and immersed in water. In Rio Oil And Gas Expo And Conference. https://doi.org/10.48072/2525-7579.rog.2020.199

Del Vecchio, C. J. M. (1992). Light weight materials for deep water moorings (PhD Thesis, University of Reading).

Duarte, J. P., Guilherme, C. E. M., da Silva, A. H. M. F. T., Mendonça, A. C., & Tempel Stumpf, F. (2019). Lifetime prediction of aramid yarns applied to offshore mooring due to purely hydrolytic degradation. *Polymers and Polymer Composites, 27*(8), 518-524. https://doi.org/10.1177/0967391119851386

Emri, I., Nikonov, A., Zupančič, B., & Florjančič, U. (2008). Time-dependent behavior of ropes under impact loading: A dynamic analysis. *Sports Technology, 1*(4-5), 208-219. https://doi.org/10.1080/19346182.2008.9648475

Gilat, A., & Subramaniam, V. (2009). Métodos numéricos para engenheiros e cientistas: uma introdução com aplicações usando o MATLAB. Bookman Editora.

International Organization for Standardization. (2005). 139 Textiles — Standard atmospheres for conditioning and testing. ISO: Geneva.

International Organization for Standardization. (2009). 2062 Textiles — Yarns from packages — Determination of singleend breaking force and elongation at break using constant rate of extension (CRE) tester. ISO: Geneva.

Jacques, B., Werth, M., Merdas, I., Thominette, F., & Verdu, J. (2002). Hydrolytic ageing of polyamide 11. 1. Hydrolysis kinetics in water. *Polymer, 43*(24), 6439-6447. https://doi.org/10.1016/S0032-3861(02)00583-9

Ma, Y., Jin, S., & Zhang, S. (2018). Effect of trigger on crashworthiness of unidirectional carbon fibre reinforced polyamide 6 composites. *Plastics, Rubber and Composites, 47*(5), 208-220. https://doi.org/10.1080/14658011.2018.1466502

McKenna, H. A., Hearle, J. W. S., & O'Hear, N. (2004). Handbook of fibre rope technology (Vol. 34). Woodhead publishing.

McLaren, A. J. (2006). Design and performance of ropes for climbing and sailing. *Proceedings of the institution of mechanical engineers, Part L: Journal of Materials: Design and Applications, 220*(1), 1-12. https://doi.org/10.1243/14644207JMDA75

Militký, J., Venkataraman, M., & Mishra, R. (2018). The chemistry, manufacture, and tensile behavior of polyamide fibers. In Handbook of properties of textile and technical fibres (pp. 367-419). Woodhead Publishing. https://doi.org/10.1016/B978-0-08-101272-7.00012-2

Montgomery, D. C., & Runger, G. C. (2012). Estatística aplicada e probabilidade para engenheiros. Rio de Janeiro: LTC Editora, 2012 (5ª Edição).

Najafi, M., Nasri, L., & Kotek, R. (2017). High-performance nylon fibers. In Structure and properties of high-performance fibers (pp. 199-244). Woodhead Publishing. https://doi.org/10.1016/B978-0-08-100550-7.00009-7

Nikonov, A., Saprunov, I., Zupančič, B., & Emri, I. (2011). Influence of moisture on functional properties of climbing ropes. *International Journal of Impact Engineering, 38*(11), 900-909. https://doi.org/10.1016/j.ijimpeng.2011.06.003

Rudman, M., & Cleary, P. W. (2016). The influence of mooring system in rogue impact on an offshore platform. *Ocean engineering, 115*, 168-181. https://doi.org/10.1016/j.oceaneng.2016.02.027

Schwertman, N. C., Owens, M. A., & Adnan, R. (2004). A simple more general boxplot method for identifying outliers. *Computational statistics & data analysis, 47*(1), 165-174. https://doi.org/10.1016/j.csda.2003.10.012

Sozen, B., Coskun, T., & Sahin, O. S. (2023). Dynamic characterization and damage analysis for the thermoplastic fiber-reinforced epoxy composites exposed to repeated low velocity impact. *Journal of Thermoplastic Composite Materials*, 08927057231223927. https://doi.org/10.1177/08927057231223927

Wang, H. (2022). Taut mooring. In Encyclopedia of Ocean Engineering (pp. 1933-1937). Singapore: Springer Nature Singapore. https://doi.org/10.1007/978-981-10-6946-8_146

Weller, S. D., Johanning, L., Davies, P., & Banfield, S. J. (2015). Synthetic mooring ropes for marine renewable energy applications. *Renewable energy, 83*, 1268-1278. https://doi.org/10.1016/j.renene.2015.03.058

Williamson, D. F., Parker, R. A., & Kendrick, J. S. (1989). The box plot: a simple visual method to interpret data. *Annals of internal medicine, 110*(11), 916-921. https://doi.org/10.7326/0003-4819-110-11-916

Appendix A

In this **Appendix A**, the respective boxplots of the statistical filtering performed on the impact cycle rupture data for polyamide under hydrolysis conditions are presented. **Fig. A1** corresponds to the loading condition of 3% of the YBL, **Fig. A2** to the loading condition of 4% of the YBL, **Fig. A3** to the loading condition of 5% of the YBL, **Fig. A4** to the loading condition of 6% of the YBL, and **Fig. A5** to the loading condition of 7% of the YBL.

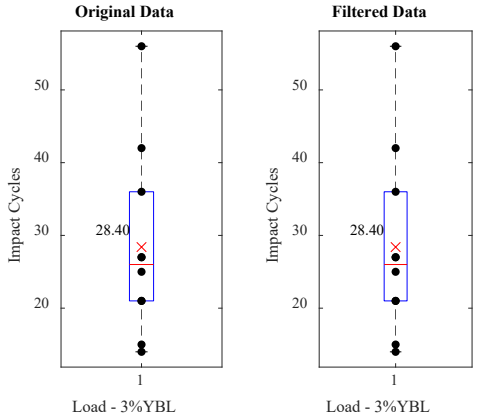

Fig. A1. Box plot with original and filtered data, 3% YBL

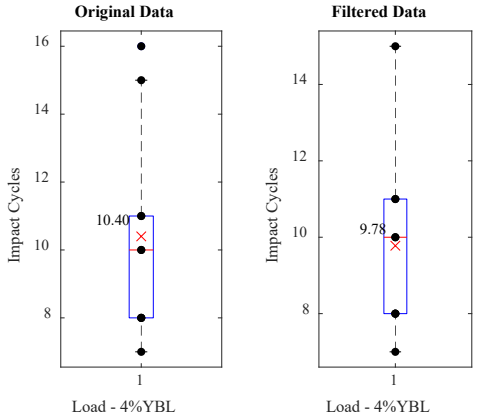

Fig. A2. Box plot with original and filtered data, 4% YBL

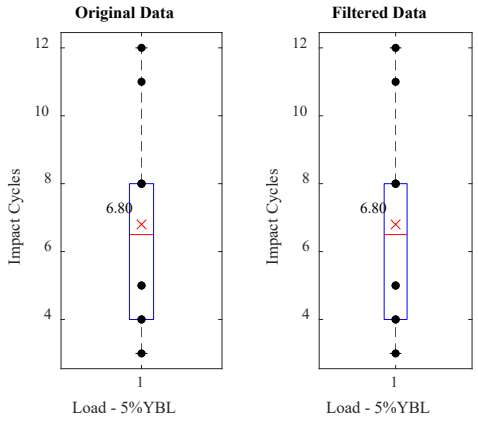

Fig. A3. Box plot with original and filtered data, 5% YBL

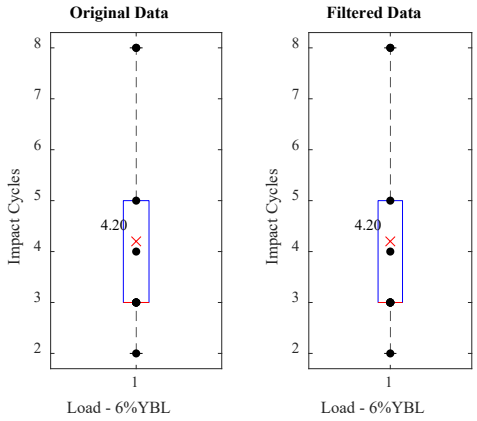

Fig. A4. Box plot with original and filtered data, 6% YBL

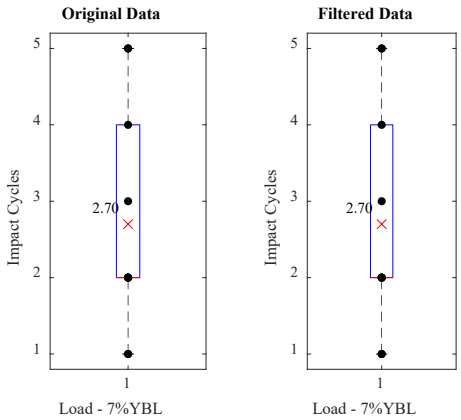

Fig. A5. Box plot with original and filtered data, 7% YBL

© 2025 by the authors; licensee Growing Science, Canada. This is an open access article distributed under the terms and conditions of the Creative Commons Attribution (CC-BY) license (http://creativecommons.org/licenses/by/4.0/).